

Lasers in Manufacturing Conference 2017

## Rotary 2.5D pulsed laser ablation

Maximilian Warhanek<sup>a,\*</sup>, Josquin Pfaff<sup>a</sup>, Johannes Gysel<sup>a</sup>, Konrad Wegener<sup>a</sup>

<sup>a</sup>*Institute of Machine Tools and Manufacturing, ETH Zurich, Switzerland*

---

### Abstract

2.5D volume ablation, i.e. the layer-by-layer material removal of three-dimensional geometries by pulsed laser ablation, is a widespread process applied in research and industry. It allows for the manufacturing of concave geometries with little constraints regarding geometric complexity, dimension and workpiece material. This has expanded the limits of modern manufacturing capabilities especially for micro-features with challenging accessibility and the shaping of hard to machine, brittle and ultrahard materials, such as diamond.

This paper presents the extension of 2.5D volume ablation process to rotary workpieces. While planar 2.5D volume ablation strategies are subject of extensive research and are supported by a variety of commercial hardware and software solutions already, rotary applications are limited. To date, e.g. the helical grooves on drilling tools or threads are processed by stitching planar 2.5D volume segments at different rotary positions. The process-efficiency can be improved and possible irregularities at the stitching areas can be avoided by continuous cylindrical layer-by-layer material removal.

A number of different strategies are analyzed with regards to processing time considering the different dynamic constraints of mechanical and scanner axes. A synchronized control setup for the rotary motion of a cylindrical workpiece and the scanning motion of the optical axes is implemented to enable the favored strategy. Furthermore, a comprehensive software tool for the generation of laser-beam paths from the CAD data of arbitrary rotary workpieces is implemented.

Experiments show the functionality of hardware and software for rotary 2.5D pulsed laser ablation. The processing results validate the applicability of the chosen scanning strategy and show significant reduction in processing time compared to according stitching processes.

Keywords: Pulsed-laser ablation, computer-aided manufacturing;

---

### 1. Introduction

Pulsed-laser ablation has reached a high level of industrial maturity. Initial applications started in the fields of laser marking, as reviewed by Noor et al., 1994, and laser surface structuring, as applied by Conrad and Richter, 2014. In recent years, the technology is increasingly applied in combination with ultrashort-

---

\* Corresponding author. Tel.: +41 44 633 21 48  
E-mail address: warhanek@iwf.mavt.ethz.ch

pulsed laser sources for the generation of three-dimensional concave features in difficult-to-machine materials, such as industrial ceramics or diamonds. This is achieved by so-called 2.5D volume ablation, thus the layer-by-layer material removal by scanning the laser focus over the target surface, as discussed by Neuenschwander et al., 2014. For all named applications, computer-aided manufacturing (CAM) software is required for the efficient generation of beam paths according to the workpiece geometry and laser scanning strategy. Commercial CAM systems for the calculations of beam paths for 2.5D volume ablation are available, e.g. SCAPS SAMLight or CAM service CAGILA. These typically are fully integrated with laser scanner controls and provide comprehensive functionalities. Fig 1 illustrates the two main processes performed by these tools. First, the target volume is sliced into the two-dimensional layers that are ablated subsequently. Second, a hatch of laser beam paths is generated to fill each layer.

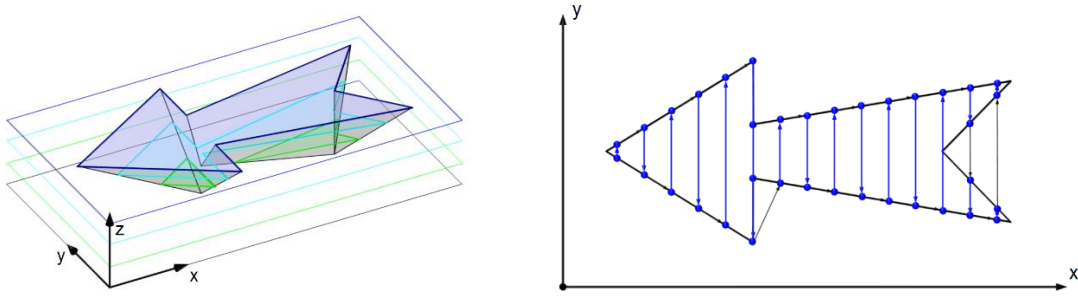


Fig. 1. (left) Slicing of the ablated volume; (right) beam-path generation for one layer

The entire 3D geometry is typically generated solely by a laser scanning setup. Supplemented with a focus shifting telescope, a galvanometer scanner is able to perform the beam paths of each layer while compensating for the changing distance of the workpiece surface from the focusing optics. 3D geometries on multiple sides of a complex workpiece or larger than the working area of the scanner, are typically produced by stitching. CNC axes, with a separate motion controller are used only for the purpose of positioning the workpiece relative to the scanner to reach the different areas on the surface. Butler-Smith et al., 2012, presented a solid diamond micro-grinding tool generated by this strategy. After completion of each staggered row of abrasive features, the tool was rotated by an indexing stage.

Modern CNC controls allow for synchronized motion of mechanical CNC axes and galvanometer scanners. This opens new degrees of freedom for laser processing strategies. Amongst others, the 2.5D volume ablation process can be applied to workpieces larger than the scanning field without interrupting the scanning motion. This eliminates the necessity of stitching methods and potential defects at the transition zones. Further, it enables the application of 2.5D volume ablation with cylindrical layers processed without interruption. This shall reduce processing time and increase workpiece quality through the elimination of transition areas. As no available CAM system supports appropriate laser scanning strategies for rotary 2.5D volume ablation, this work provides the basis for the beam path calculation and a prove of concept.

## 2. Computer-aided manufacturing for rotary 2.5D pulsed-laser ablation

### 2.1. Process considerations

Fig 2 shows six different approaches to rotary 2.5D volume ablation. The different scanning strategies vary strongly with regards to the distribution of the laser scanning motion between a rotary axis and a linear axis.

Because the linear motion can be performed by a galvanometer scanner, which allows for significantly higher dynamics, while the rotary axis may reach high speed but is limited in acceleration, the theoretical processing speed of these strategies differ strongly. Due to the different degrees of freedom with regards to scanning direction variation between layers, the strategies may also result in different surface quality. It is assumed that best quality can be achieved by changing the scanning direction after each layer.

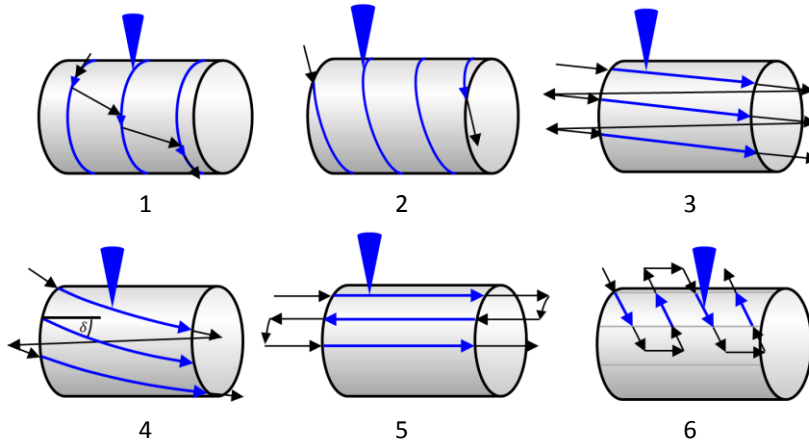


Fig. 2. Six scanning strategies for rotary 2.5D volume ablation; blue arrows: laser scanning motions; black arrows: jump motions with laser switched off

1. The first strategy achieves high scanning speed by fast rotation of the workpiece. With the appropriate hardware, high removal rates can be achieved. Little to no variation of the scanning direction between two layers is possible, which may be detrimental to the surface quality.
2. Strategy 2 is similar to strategy 1. By applying a spiral hatch motion the jump movements of strategy 1 are eliminated. This should enable slightly higher processing speed, but requires a linear axis synchronized to the fast rotary motion.
3. The third strategy moves the main portion of the motion to the linear axis, which can be a highly dynamic galvanometer scanner axis. The angular variation of the scanning direction is limited. High removal rates are possible with this strategy, but a synchronous CNC control of mechanical and scanning axes is required.
4. Strategy 4 solves the issue of limited angular variation by skipping scans and finishing a layer in multiple rotations. This allows for higher angular variation of the scanning direction and superior surface quality.
5. The fifth strategy is limited to scans parallel to the rotary axis. This gives the advantage that no synchronized motion of the linear and the rotary axis is required. The rotary motion could be performed by a stepper motor. However, the consecutive scanning and rotating motions are significantly slower than the synchronized strategies. Also, grooves parallel to the scanning direction are to be expected because the scanning direction is not varied.
6. For the sake of completeness, a stitching strategy is mentioned. Strategy 6 are conventional planar 2.5D volume ablation patches, which are processed consecutively. The rotary axis is only used for positioning purposes. Irregularities in the workpieces surface at the transition areas are to be expected.

Strategies 3 and 4 are considered the most beneficial for high workpiece quality and high removal rate. They combine a continuous rotary motion of the workpiece with a linear scanning motion, as illustrated in Fig 3. Key to the generation of the target geometry is the synchronized gating, i.e. fast modulation of the laser power, according to the rotary and scanner axis position. The following sections give an overview of the NC-code generation for this purpose and show some validation experiments.

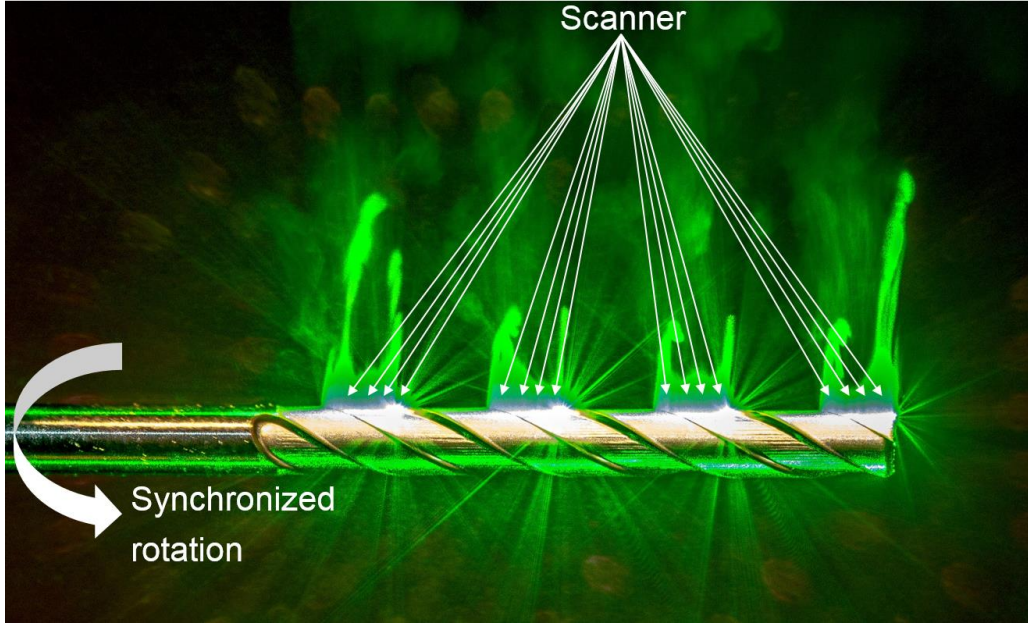


Fig. 3. Rotary 2.5D volume ablation of a helical drilling tool.

## 2.2. Programming Structure

In the following, the sequential tasks to be performed for rotary pulsed laser ablation are discussed. Fig 4 illustrates the preparation of the CAD drawing of the target geometry. The ablated volume is the Boolean subtraction of the target geometry from the blank. For this implementation, it is necessary to convert the 3D data of the volume to be ablated into the STL format, which defines a body by surface triangles and outer normal. The Cartesian coordinates of each vertex, i.e. corner point, of each surface triangle of the ablated volume are therefore known. The rotation axis of the workpiece must be aligned with the X-axis in the CAD drawing.

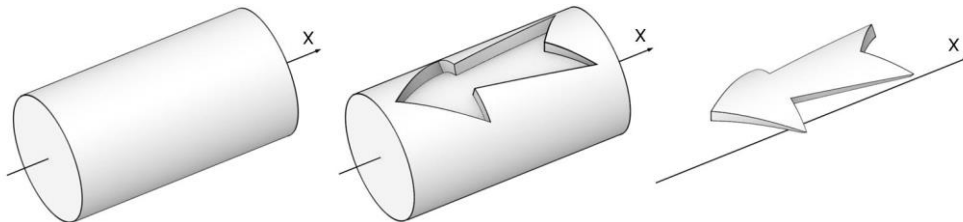


Fig. 4. (left) blank workpiece; (middle) target geometry; (right) ablated volume

The second step, illustrated in Fig 5, unrolls the ablated volume for easier scan path calculation. For this purpose, the 3D coordinates of the vertices are transformed in cylindrical coordinates and then transformed according to

$$\begin{aligned}
 x' &= x \\
 y' = \varphi &= \begin{cases} \arctan(z/y) + 90^\circ & \text{if } y \leq 0 \\ \arctan(z/y) + 270^\circ & \text{if } y > 0 \end{cases} \\
 z' = r &= \sqrt{y^2 + z^2}
 \end{aligned} \tag{1}$$

The new representation of the geometry equals a Cartesian coordinate system with the Y-axis representing the *unrolling angle*  $\varphi$  [°]. This representation allows for application of the same algorithms for the slicing and the beam path calculation as applied for conventional planar 2.5D volume ablation.

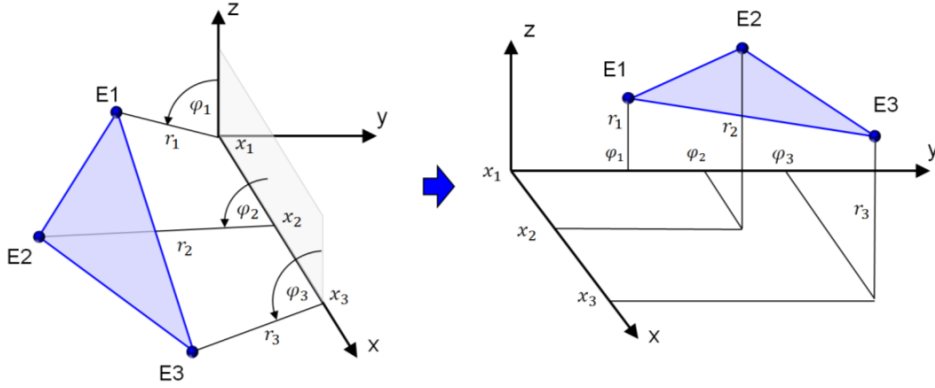


Fig. 5. (left) surface triangle before transformation; (right) surface triangle after transformation

The next step is the slicing of the geometry to generate the individual layers to be processed. As this step is identical to planar 2.5D volume ablation it needs no further discussion. After the slicing, the beam paths filling each layer are calculated. Due to the strongly varying dynamic properties of scanner axis and rotary axis, limitations with regard to the line distance and the hatch angle are considered. These, limitations also vary for each layer, as the surface speed achieved by the same rotational speed is reduced with decreasing workpiece radius. Fig 6 shows the transformation applied to compensate for the warping of the layer due to the rotation of the workpiece during one linear scan. To achieve homogeneous processing results, the line distance is adapted to achieve an integer number of lines for each rotation. The resulting minor variation of the ablated volume in this layer can be compensated by adapting the scanning speed or the layer thickness.

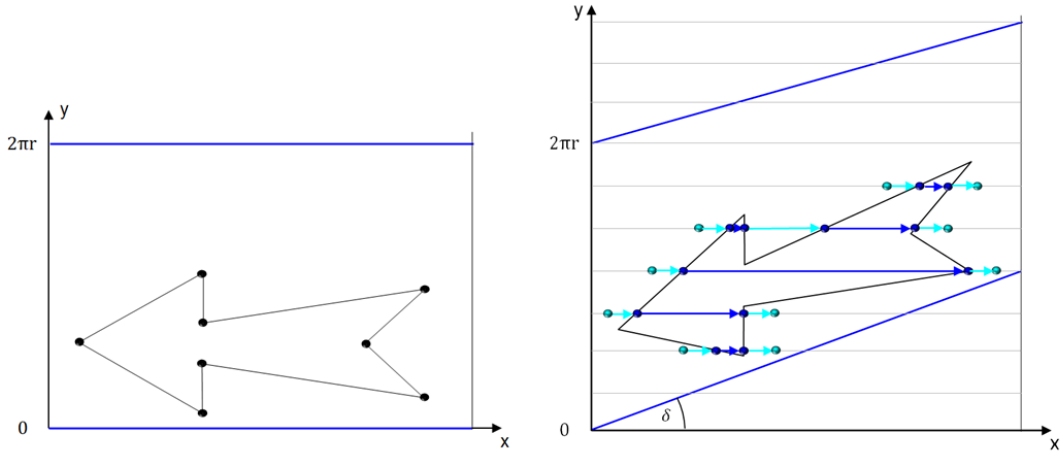


Fig. 6. (left) contour of one slice; (right) transformed contour with scan paths considering the rotational motion of the workpiece synchronous to the scanning motion

As for planar 2.5D volume ablation, a number of strategies for the optimization of the processing results can be applied. These cover:

- the calculation of skywriting lines, which allow for constant scanning speed during one line by accelerating and decelerating while the laser is switched of,
- the calculation of contour offsets to compensate for the effective focus radius,
- and variation of the hatch angle after each layer to reduce the formation of grooves parallel to the scanning direction caused by the accumulation of the parabolic ablation profiles generated by a Gaussian beam distribution. The angle variation is limited by the speed ratio between the achievable surface speed of the rotary axis and the applied scanning speed by the scanner axis.

Fig 7 gives illustrations of these three options. Finally, the calculated beam paths are converted into the NC-code required for the individual setup.

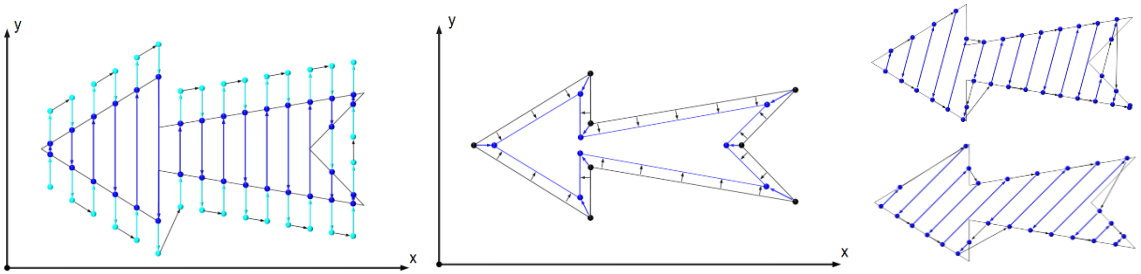


Fig. 7. (left) skywriting; (middle) contour offset; (right) hatch angle variation

### 2.3. Implementation and Validation Experiments

The discussed CAM system is prototypically implemented in MATLAB. To support the application of the CAM functionalities and choice of strategies, a graphical user interface is added, as shown in Fig 8.

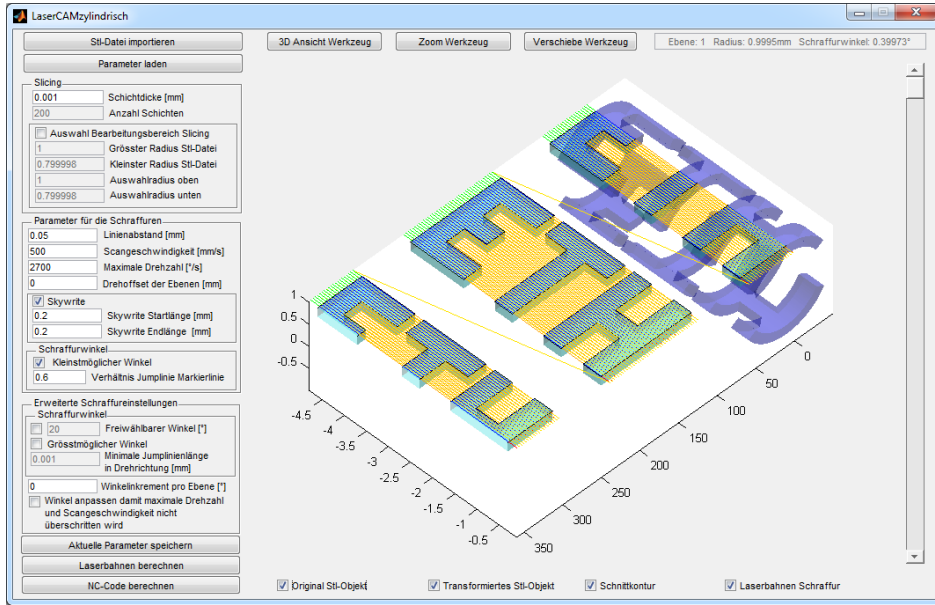


Fig. 8. Graphical user interface of the MATLAB implementation

The manufacturing of a Zirconia oxide dental implant is chosen as demonstrator for the CAM implementation. The CAD drawing of a ZERAMEX T ZERALOCK type T16308 implant is successfully loaded into the CAM system. The geometry has a diameter of 4.2 mm and a length of 9.6 mm. The CAM calculates 274 slices and about 5.7 million lines of NC code in 4 min on a consumer-grade notebook. Fig 9 shows the ablated volume and the unrolled geometry with one layer.

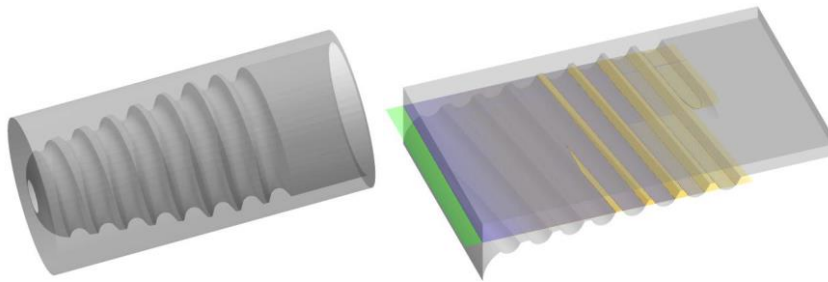


Fig. 9. (left) CAD drawing of the ablated volume for a dental implant; (right) unrolled ablation geometry with beam paths indicated for one layer: green: acceleration paths, blue: scan paths, yellow: jump paths.

To test the code an appropriate setup based on an Aerotech A3200 control, a rotary axis and a galvanometer scanner is applied. The control enables fully synchronized motion of the rotary axis and the scanner. The laser source emits pulses with a length of 400 fs, a wavelength of 520 nm and a pulse energy of 10  $\mu$ J. Fig 10 shows the processing result. After some minor adjustments of the processing strategy within the scope of the CAM tool functionality, such as variation of line distance and skywriting parameters, a satisfactory implant is produced. The processing time is approximately 2.5 h. Measurements show, that the average contour deviation is below 20  $\mu$ m, which is in a similar range to the conventional manufacturing



process. Higher precision should be achievable by choosing a lower layer thickness, which in this case is set to  $7.2\text{ }\mu\text{m}$ . The surface roughness at the base of the helical grooves is measured with a Leica DCM 3D confocal microscope to be  $R_a = 0.7\text{ }\mu\text{m}$  and  $R_z = 3.7\text{ }\mu\text{m}$  with a cutoff wavelength of  $\lambda_c = 0.8\text{ mm}$ . For this application, this roughness is considered to be desired for the intergrowth with bone tissue.

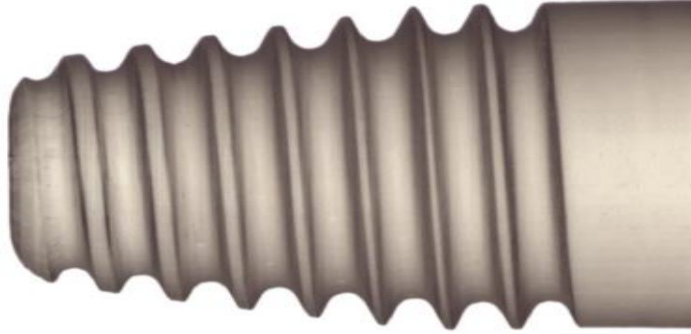


Fig. 10. Dental implant produced by rotary 2.5D volume ablation

### 3. Conclusion and Outlook

This work presents the theoretical basis for the extension of the much-applied 2.5D volume ablation processes from planar to rotary workpieces. A prototypical implementation and the production of a ceramic dental implant by the methodology prove the concept. The limiting factor is the requirement of synchronized motion of a laser scanner and a rotary axis, which is not fulfilled by most industrial CNC systems.

As only linear scanning motions are required for the presented strategy of rotary 2.5D volume ablation, the process efficiency could significantly be increased by the application of a polygon scanner, which allows for higher scanning speed and therefore higher ablation rates. However, a synchronized control of a polygon scanner and the rotary axis is not available and does not seem to be a standard solution.

### Acknowledgements

The authors thank Dentalpoint AG for making the applied laser infrastructure available and Aerotech Inc. for the continued support during the implementation of new strategies on their motion controllers.

### References

- Butler-Smith, P., Axinte, D., Daine, M., 2012. Solid diamond micro-grinding tools: From innovative design and fabrication to preliminary performance evaluation in Ti-6Al-4V, *International Journal of Machine Tools & Manufacture* 59, p. 55-64.
- Conrad, D., Richter, L., 2014, Ultra-short pulse laser structuring of molding tools, *Physics Procedia* 56, p. 1041-1046.
- Neuenschwander, B., Jaeggi, B., Schmid, M., Hennig, G., 2014. Surface structuring with ultra-short laser pulses: Basics, limitations and needs for high throughput, *Physics Procedia* 56, p. 1047-1058.
- Noor, Y., Tam, S., Lim, L., Jana, S., 1994. A review of the Nd:YAG laser marking of plastic and ceramic IC packages, *Journal of Materials Processing Technology* 42, p. 95-133.